Brief Communication

α-Band oscillations in intracellular membrane potentials of dentate gyrus neurons in awake rodents

Ross W. Anderson[1] and Ben W. Strowbridge[1,2]

[1]Department of Physiology and Biophysics, [2]Department of Neurosciences, Case Western Reserve University School of Medicine, Cleveland, Ohio, USA

The hippocampus and dentate gyrus play critical roles in processing declarative memories and spatial information. Dentate granule cells, the first relay in the trisynaptic circuit through the hippocampus, exhibit low spontaneous firing rates even during locomotion. Using intracellular recordings from dentate neurons in awake mice operating a levitated spherical treadmill, we found a transient membrane potential α-band oscillation associated with the onset of spontaneous motion, especially forward walking movements. While often subthreshold, α oscillations could regulate spike timing during locomotion and may enable dentate gyrus neurons to respond to specific cortical afferent pathways while maintaining low average firing rates.

[Supplemental material is available for this article.]

Many diverse brain activity states are associated with network oscillations, typically recorded using field potential electrodes or by following the spiking activity of many neural units simultaneously (Buzsáki et al. 1983; Buzsáki 2010). Movement-related oscillations have been studied in a variety of species, especially in rodents which display place-related neural information that can be decoded by analyzing spike timing within nested θ and γ-band oscillations (O'Keefe 1976; Buzsáki 2010). Little is known, however, about the specific pattern of subthreshold membrane potential modulation—reflecting the synaptic input and the specific intrinsic electrophysiological properties of each neuron—that gives rise to the pattern of spiking output in behaving animals. The intracellular correlate of network oscillations is of special interest in the dentate gyrus (DG) where most neurons maintain very low average firing rates despite robust modulation by locomotion-related oscillations (Neunuebel and Knierim 2012).

The recent application of patch-clamp recording methods to awake, head-fixed rodents (Harvey et al. 2009) has enabled direct recording of membrane potential modulation during many behaviors, including locomotion. Through recording intracellular potentials in DG neurons during short spontaneous movements, we found evidence for transient subthreshold α-band oscillation associated with movement onset that modulates firing probability. By continuously varying the intracellular membrane potential, subthreshold oscillations likely play an important role in maintaining sparse firing patterns in output neurons while enabling integration of information from cortical afferent pathways.

We recorded from 18 DG neurons with overshooting action potentials (APs) using blind whole-cell patch-clamp methods in awake mice that were conditioned to be head-restrained on a spherical treadmill (Harvey et al. 2009; Youngstrom and Strowbridge 2012) to assess intracellular responses during epochs of spontaneous movement (see Supplemental Methods for details). While these data set likely contained dentate granule cells and interneurons, the relatively low yield of recovering dye-filled neurons and overlapping intrinsic properties precluded a robust classification of presumptive cell classes. Both successfully recovered neurons from this study were located in the granule cell layer. We, therefore, analyzed spontaneous motion-related membrane potential responses in all recorded neurons grouped together. Most recordings were obtained with a depolarizing bias current applied to promote a low frequency of spontaneous spiking (1.6 ± 0.3 Hz; $n = 18$ cells from 13 mice). Without applied bias current, dentate gyrus neurons fired infrequently (0.12 ± 0.08 Hz; RMP $= -66.0 \pm 2.7$ mV).

In this study, we analyzed 23 spontaneous movement epochs from 11 neurons. (No spontaneous movements lasting >2 sec occurred in the other seven intracellular recordings.) Membrane potential fluctuations increased during all 23 spontaneous movement epochs analyzed (duration range 2–22 sec; mean 7.5 ± 1.0 sec). These fluctuations did not appear to reflect mechanical instability since there was little drift in the average membrane potential following the movement (-0.23 ± 0.6 mV, compared with premovement membrane potential; not significantly different from 0; $P = 0.72$). Increases in membrane potential variance also preceded detectable motion in multiple epochs. Mean membrane potential variance increased from 11.4 ± 2.0 to 20.9 ± 4.4 mV^2 in the 250-msec window immediately before detectable movement (means significantly different, $t_{(22)} = -2.43$; $P < 0.05$; $n = 23$; paired *t*-test).

The onsets of spontaneous movement epochs often were accompanied by a brief period of α-band activity in intracellular recordings from DG neurons. In the 18-sec movement epoch shown in Figure 1A, the initial α-band activity lasted for ~500 msec (black horizontal bar in Fig. 1A) and was followed 13.3 sec later by large-amplitude θ-band modulation in the membrane potential and spike output (gray bar). Figure 1B shows an enlargement containing α-band modulation from the example presented in Figure 1A. Similar α-band oscillations associated with the onset of a spontaneous movement in a different DG neuron is shown in Figure 1C. In this example, α-band modulation was associated

Corresponding author: bens@case.edu
Article is online at http://www.learnmem.org/cgi/doi/10.1101/lm.036269.114.

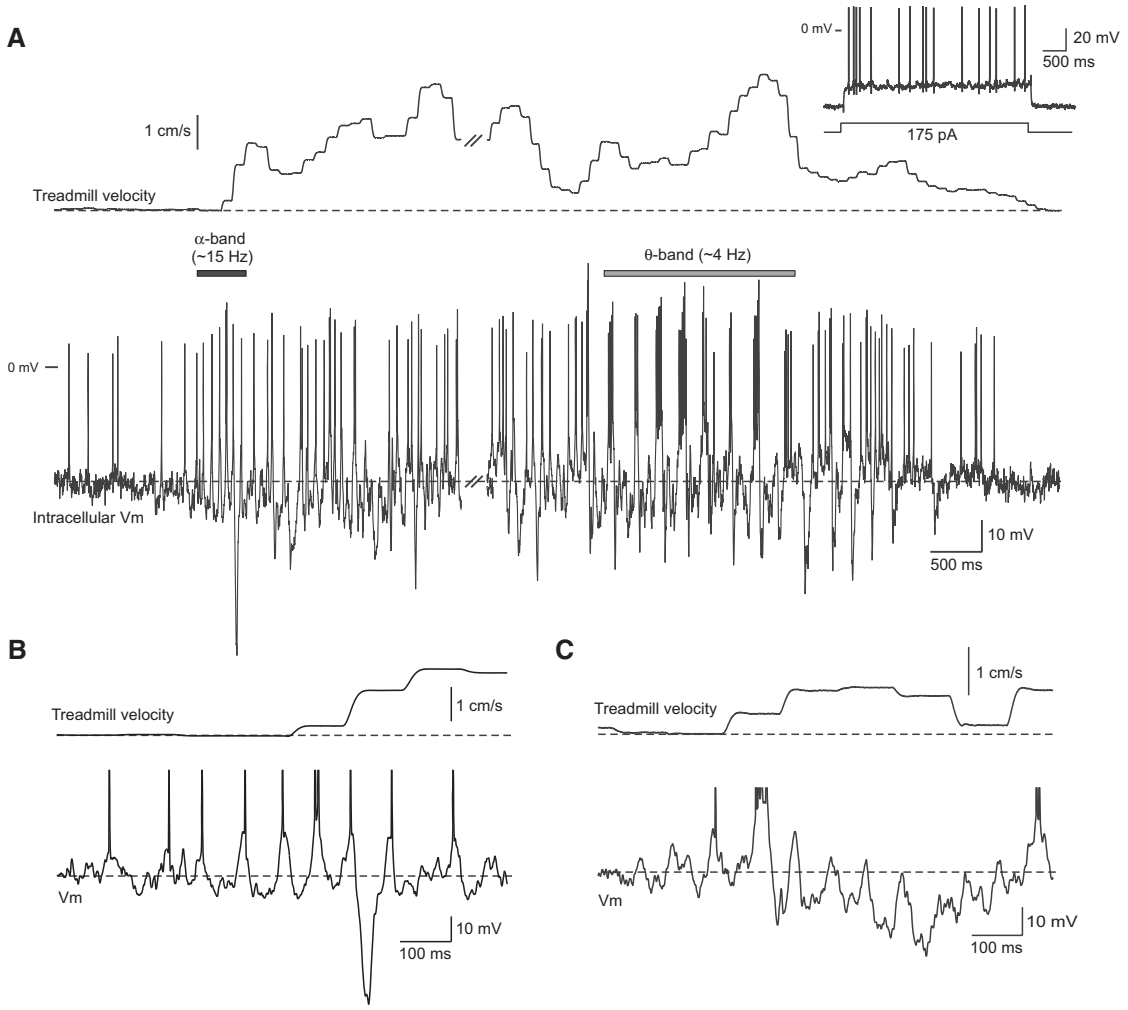

Figure 1. Intracellular response recorded during a spontaneous movement epoch. (*A*) Simultaneous recording of intracellular membrane potential in a dentate gyrus neuron (*bottom* trace) and spherical treadmill velocity (combined forward/backward and rotational axes) during a spontaneous movement epoch (18-sec duration; traces interrupted at double slash mark). Intracellular recording example shows both α-band membrane potential modulation near movement onset (horizontal black bar) and θ-band modulation (gray bar) later during the epoch. *Inset* shows response to a depolarizing current step in the same neuron. (*B*) Enlargement of the α-band membrane potential modulation from the example epoch shown in *A*. (*C*) Similar α-band membrane potential modulation recorded during movement onset in a different dentate gyrus neuron. Action potentials truncated in *B* and *C*.

with a hyperpolarizing shift in the membrane potential with only three oscillation cycles triggering APs.

While membrane potentials followed complex trajectories during most of the movement epochs, the early α-band oscillation and subsequent periods of θ-band activity were common in the cell population analyzed in this report. Since θ-band modulation has been reported previously (O'Keefe and Recce 1993; Ylinen et al. 1995; Skaggs et al. 1996), the present report is focused on the initial α-band modulation. The complexity of synaptic events recorded under current clamp, and the inability to record similar spontaneous movements while holding neurons at different membrane potentials, precludes analyzing individual synaptic responses in this study. In particular, determining whether rapid membrane hyperpolarizations present in many DG recordings (e.g., Fig. 1B) represent intrinsic after hyperpolarization responses or large-amplitude inhibitory synaptic potentials will likely require voltage clamp methods and focal extracellular stimulation and will be addressed in a subsequent study.

The α-band membrane oscillations often began before treadmill motion was detected, as illustrated in the spectrogram in Figure 2A. The α-band intracellular response in this example was evident 460 msec before treadmill motion was detected, suggesting this oscillation may be associated with preparatory neural activity. The increase in α-band power with motion onset also was evident in summary analysis from multiple neurons. Power spectra computed from the 18 spontaneous movements encompassing distances >3 cm showed a peak at α-band (at 13.4 Hz in the middle plot in Fig. 2B). The spectra computed 1 sec later from the same episodes had a prominent peak in the θ-band (7.3 Hz in the *bottom* plot in Fig. 2B). The average duration of the α-band oscillation evident in spectrograms was 2.0 ± 0.3 sec ($n = 18$). Integrating power spectra from 8 to 15 Hz also revealed a large increase in α-band membrane potential modulation with movement onset and a smaller but statistically significant increase in α-band power 1 sec before detectable movement (Fig. 2C). Average θ-band (4–7 Hz) power was increased as the movement developed but was not statistically enhanced before detectable movement (Fig. 2D). There was no increase in mean α-band power at the onset of the five spontaneous movements that encompassed distances <3 cm (-0.55 ± 0.2 in the same scale presented in Fig. 2B).

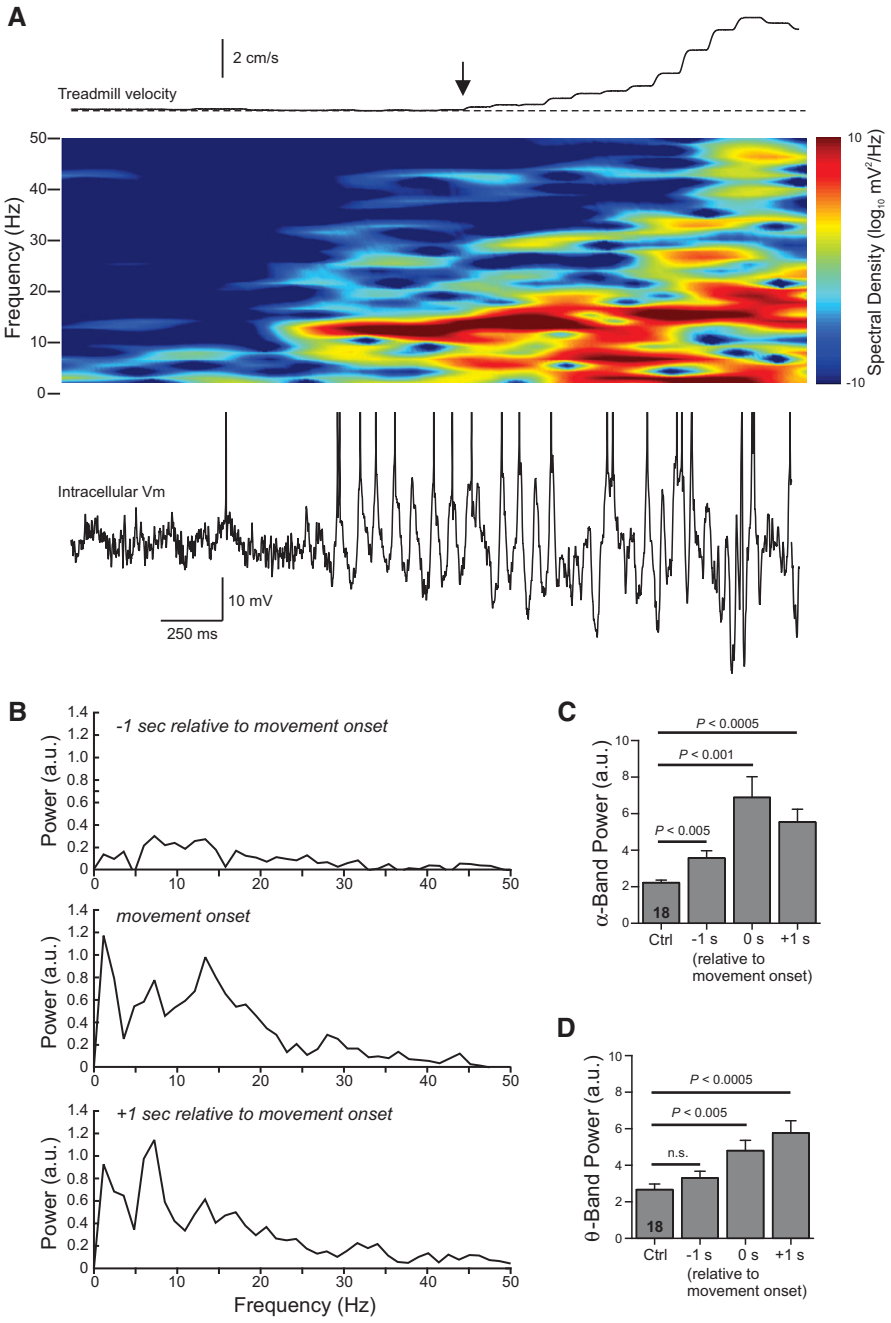

Figure 2. Spectral analysis of intracellular responses during movement onset. (*A*) Spectrogram computed from the membrane potential during a 3-sec duration window that included the onset of a spontaneous movement epoch (*vertical arrow*). Combined treadmill velocity plotted *above* spectrogram. Action potentials truncated in example trace shown. (*B*) Average power spectra computed from 18 spontaneous movement epochs >3 cm from 10 cells during the three 812-msec time windows indicated *above* each plot. The power spectrum coincident with movement onset showed a primary peak in the α-band (13.4 Hz). The primary peak shifted to the θ-band (7.3 Hz) in the spectrum computed 1 sec following movement onset. (*C*) Plot of the integrated spectral power with the α-band (8–15 Hz) during quiescent periods (*Ctrl*) and during movement onset (same three time windows analyzed in *B*). The average α-band power significantly increased over control levels in all three time windows, including the window that started 1 sec before detectable movement. Repeated-measures ANOVA ($F_{(3,51)} = 15.09$, $P < 5 \times 10^{-7}$) followed by paired *t*-test with a Bonferroni correction of 3; $n = 18$ epochs. (*D*) Plot of the integrated spectral power during the θ-band (4–7 Hz) for the same spontaneous movement epochs analyzed in B and C. Average θ-band power was not significantly elevated before the movement onset ($P = 0.06$; paired *t*-test) but was immediately after the movement began. Repeated-measures ANOVA ($F_{(3,51)} = 12.86$; $P < 5 \times 10^{-6}$); $n = 18$ epochs.

Intracellular α-band power was more strongly correlated with treadmill motion along the axis engaged by forward and backward movement (Fig. 3A; $R = 0.62$; $F_{(1,21)} = 13.34$; $P < 0.002$) than rotational motion (Fig. 3B; $R = -0.02$; $P = 0.93$). This result suggests that the strong increase in membrane potential variance with motion along the forward/backward axis noted above likely reflects α-band membrane potential oscillations. The complexity of the treadmill motion during spontaneous movement epochs—often involving both forward walking and reverse treadmill motion—precluded analysis of the relative contribution of each movement direction to the membrane potential oscillation. The magnitude of the α-band oscillation during the initial 2 sec of motion was strongly correlated with the duration of the movement epoch ($R = 0.76$; $F_{(1,21)} = 27.98$; $P < 10^{-4}$; Fig. 3C).

Even with added depolarizing bias current, DG neurons recorded in this study spiked relatively infrequently during the α-band oscillation (mean 0.38 spikes/cycle during the initial 2 sec of spontaneous movements). In movement epochs encompassing >3 cm and spontaneous firing prior to the movement, the average firing rate did not change during the initial 2 sec of the movement epoch (96.7 ± 32% of premovement spiking frequency; $n = 15$ epochs from nine cells with spontaneous spiking; $P = 0.82$). However, the α-band membrane potential oscillation strongly modulated spike timing during movement onset. The distribution of spike times relative to α-band oscillation peaks (Fig. 3D1–2) was strongly peaked near 0-msec delay (2.6 ± 0.6 msec). There was no spike/oscillation coupling when the same data set was analyzed following trial shuffling (e.g., comparing spike times in one episode with oscillation peak times from another episode that also triggered APs; Fig. 3D3). These results demonstrate that while often subthreshold, the α-band oscillation in DG neurons associated with movement onset can entrain spike output.

The present study used intracellular recordings to examine the subthreshold responses of DG neurons in awake rodents operating a levitated spherical treadmill. We made three principal findings in this report. First, intracellular recordings revealed that subthreshold membrane potential fluctuations occurred near the onset of spontaneous bouts of movement and could precede the detectable movement onset by >100 msec. Second, α-band membrane potential oscillations often occurred

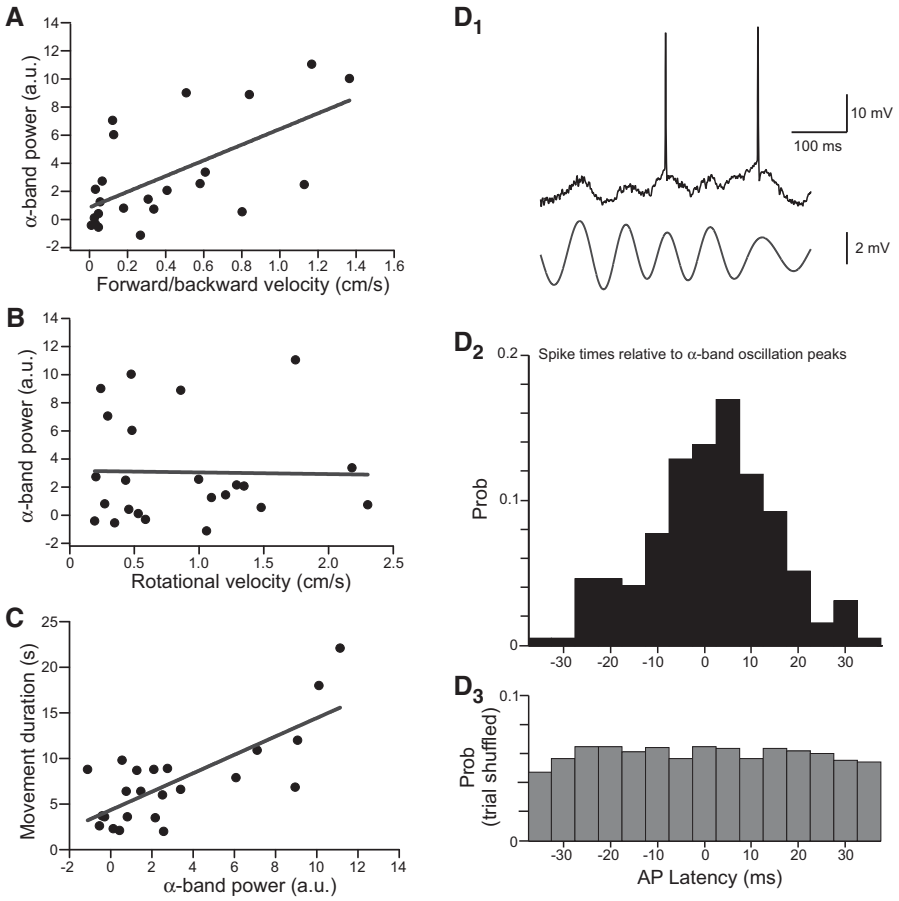

Figure 3. Properties of α-band oscillations. (*A*) Plot of the relationship between forward/backward treadmill velocity and integrated α-band power (8–15 Hz) calculated over the initial 2 sec of the movement epoch. Solid line is linear regression. $R = 0.62$. (*B*) Plot of the relationship between rotational velocity and integrated α-band power. $R = -0.02$. (*C*) Plot of the relationship between α-band power and the duration of the movement epoch. $R = 0.76$. Plots in A–C from 23 movement epochs over 11 DG neurons. (*D*1) Example intracellular recording during movement onset (*top* trace) and bandpass-filtered membrane potential (8–15 Hz; *bottom* trace). (*D*2) Histogram of relative timing between APs and α-band membrane potential oscillation cycles computed from 195 spikes recorded in 23 movement epochs from 11 dentate gyrus neurons. Latencies measured from most depolarized phase of each bandpass-filtered oscillation cycle. Mean AP latency = 2.6 msec. (*D*3) Histogram of AP synchronization with α oscillations after trial shuffling (4290 spikes/oscillation cycle latencies).

during the initial 1–2 sec of movement and were largest in movements in the forward/backward treadmill axis. Finally, the magnitude of the initial α oscillation in the membrane potential was correlated with the duration of the movement epoch, suggesting that this rhythm recorded in DG neurons may reflect, in part, synaptic input from neocortical motor planning circuits.

To our knowledge, this is the first report to use intracellular recordings to assay subthreshold oscillations in DG neurons at the onset of animal motion. While we did not attempt to classify the neurons recorded in this study, the low spontaneous firing rates we observe (0.12 ± 0.08 Hz without added bias current) are suggestive of dentate granule cells in most of our recordings. Extracellular (Rose et al. 1983; Jung and McNaughton 1993; Neunuebel and Knierim 2012) and intracellular recordings (Pernía-Andrade and Jonas 2014) from these neurons in vivo uniformly report very low rates of spontaneous firing. We observed clear α-band modulation in the membrane potential with movement onset in both neurons with low firing rates during movement epochs (e.g., Fig. 1C, a presumptive granule cell) and neurons that increased their firing with movement and exhibited rhythmic AP bursts (presumptive interneurons, e.g., Figs. 1A and 2A, based on previous extracellular recording studies; Ylinen et al. 1995; Varga et al. 2012). The presence of α-band modulation in DG neurons with diverse physiological responses suggests that this oscillation is likely present in both granule cells and interneurons.

Several groups have speculated that α rhythms during immobility represent a "ground state" that occurs in the absence of sensory input (Pfurtscheller et al. 1996; Haegens et al. 2011). α Oscillations are commonly observed in occipital cortex following eye closure (Lopes da Silva et al. 1973) and in somatosensory cortex in rodents during immobility (Buzsáki et al. 1988; Wiest and Nicolelis 2003). α Rhythms are typically abolished at the onset of movement (Pfurtscheller and Aranibar 1979; Buzsáki et al. 1983; Pfurtscheller et al. 1996) or imagined movement (Gastaut and Bert 1954).

The enhancement of α-band membrane potential modulation we find with forward/backward motion, in contrast, suggests that this predominately subthreshold oscillation mode is not widespread but, instead, is tightly linked to voluntary movement in DG neurons. The strong correlation between the magnitude of the α-band oscillation at the onset of motion and the duration of spontaneous movement epoch (Fig. 3C) is consistent with a connection to motor planning networks in parietal cortex (Pfurtscheller and Aranibar 1979; Capotosto et al. 2009; Kerr et al. 2011).

Our results are consistent with previous studies that demonstrated active functioning during periods of α oscillations (also termed β1 oscillations; Kramer et al. 2008) in extracellular recordings. Wiest and Nicolelis (2003) demonstrated that tactile stimuli could be perceived during α-band oscillations in head-fixed rodents, arguing that this oscillatory mode may be more analogous to the Rolandic μ rhythm in humans (Gastaut and Bert 1954) than a seizure-link state with damped sensory awareness, as proposed previously (Marescaux et al. 1992). In humans, the magnitude of α-band oscillations detected in premotor cortex and the supplementary motor area (Brodmann area 9) increases during working memory tasks but was not correlated with the number of memory items (Roux et al. 2012), consistent with a role of α oscillations in inhibiting potentially interfering replay events during short-term memory tasks (Hummel et al. 2002; Jensen and Mazaheri 2010). α rhythms in primate neocortex also may play a role in modulating spatial attention since trans-cranial magnetic stimulation during anticipatory α-band oscillations disrupted the identification of visual targets (Capotosto et al. 2009).

Less is known about α oscillations within the hippocampal formation than in neocortical and related thalamic areas. Nerad and Bilkey (2005) reported a consistent 10- to 12-Hz oscillation in the hippocampus and rhinal cortex of rats that was selectively enhanced in familiar environments. Similar to our findings in

intracellular recordings from DG neurons, the "flutter" rhythm reported by Nerad and Bilkey was associated with locomotion and typically occurred in brief epochs lasting 1–5 sec. The flutter rhythm appears to be distinct from the more commonly studied hippocampal θ oscillations since α-band field potential oscillations did not display a phase inversion between the stratum oriens region and the hippocampal fissure (Brankačk et al. 1993). Other investigators have raised the possibility that α-band oscillations in field potentials recorded in brain regions with large-amplitude θ rhythms, such as the hippocampus, may reflect a harmonic artifact (Buzsáki et al. 1985). This explanation is less likely in our intracellular recordings where α-band oscillations can be directly observed in the subthreshold membrane potential (e.g., Figs. 1B,C and 2A) and occurred at different times than θ-modulated spiking (e.g., Fig. 1A).

While field potential studies suggest that neocortical α oscillations are likely generated through a combination of corticocortical and thalamocortical synaptic interactions (Lopes Da Silva and Storm Van Leeuwen 1977; Lopes da Silva et al. 1980), the origins of the α oscillation we observe in the DG is less clear and could potentially include subcortical sites such as the basal ganglia or the thalamus. The α oscillations we observe in the DG have a superficial similarity to thalamic spindles, an oscillation dependent on low-threshold voltage gated Ca^{2+} channels (Steriade et al. 1993). Dentate granule cells strongly express one variant of T-type Ca^{2+} channels (α-1H; Talley et al. 1999). However, the intrinsic physiology of granule cells does not typically exhibit low-threshold Ca^{2+} spikes (Staley et al. 1992) that are typical of thalamic neurons. Alternatively, the brief epochs of α oscillations we observe in intracellular recordings may have their origin in previously established neocortical areas with strong α-band rhythms such as somatosensory and premotor cortices and are conveyed to the DG neurons through synaptic connections. Totah et al. (2009, 2013) observed preparatory α-band oscillations at ∼12 Hz several seconds before stimulus onset in prelimbic and anterior cingulate cortex, brain regions that could be the origin of the α oscillation we observe in DG neurons.

While most α oscillation cycles we recorded remained subthreshold, the firing that did occur during movement onset often was strongly modulated by the α oscillation. This finding suggests that this rhythmic modulation of the membrane potential may help enforce the sparse firing patterns associated with DG neurons (Jung and McNaughton 1993; Neunuebel and Knierim 2012) by sculpting periods of increased spike probability near the depolarized peak of each oscillation cycle. Through this mechanism, the α oscillation may enable DG neurons to respond selectively to different components of the polysensory input they receive from entorhinal cortex (Witter 2007). Jensen and Mazaheri (2010) proposed a related role for neocortical α oscillations in reducing the impact of potentially distracting neural signals. Additional studies will be required to determine which specific input modalities are regulated by α oscillations in the DG.

Acknowledgments

We thank Richard T. Pressler and Robert Hyde for constructive comments on this manuscript. This study was supported by NIH grants R01-DC04285 and R01-DC09948 to B.W.S.

References

Brankačk J, Stewart M, Fox SE. 1993. Current source density analysis of the hippocampal θ rhythm: associated sustained potentials and candidate synaptic generators. *Brain Res* **615:** 310–327.

Buzsáki G. 2010. Neural syntax: Cell assemblies, synapsembles, and readers. *Neuron* **68:** 362–385.

Buzsáki G, Lai-Wo SL, Vanderwolf CH. 1983. Cellular bases of hippocampal EEG in the behaving rat. *Brain Res Rev* **6:** 139–171.

Buzsáki G, Rappelsberger P, Kellényi L. 1985. Depth profiles of hippocampal rhythmic slow activity ('θ rhythm') depend on behaviour. *Electroencephalogr Clin Neurophysiol* **61:** 77–88.

Buzsáki G, Bickford RG, Ponomareff G, Thal LJ, Mandel R, Gage FH. 1988. Nucleus basalis and thalamic control of neocortical activity in the freely moving rat. *J Neurosci* **8:** 4007–4026.

Capotosto P, Babiloni C, Romani GL, Corbetta M. 2009. Frontoparietal cortex controls spatial attention through modulation of anticipatory α rhythms. *J Neurosci* **29:** 5863–5872.

Gasaut HJ, Bert J. 1954. EEG changes during cinematographic presentation; moving picture activation of the EEG. *Electroencephalogr Clin Neurophysiol* **6:** 433–444.

Haegens S, Händel BF, Jensen O. 2011. Top-down controlled α band activity in somatosensory areas determines behavioral performance in a discrimination task. *J Neurosci* **31:** 5197–5204.

Harvey CD, Collman F, Dombeck DA, Tank DW. 2009. Intracellular dynamics of hippocampal place cells during virtual navigation. *Nature* **461:** 941–946.

Hummel F, Andres F, Altenmüller E, Dichgans J, Gerloff C. 2002. Inhibitory control of acquired motor programmes in the human. *Brain* **125:** 404–420.

Jensen O, Mazaheri A. 2010. Shaping functional architecture by oscillatory α activity: gating by inhibition. *Front Hum Neurosci* **4:** 186.

Jung MW, McNaughton BL. 1993. Spatial selectivity of unit activity in the hippocampal granular layer. *Hippocampus* **3:** 165–182.

Kerr CE, Jones SR, Wan Q, Pritchett DL, Wasserman RH, Wexler A, Villanueva JJ, Shaw JR, Lazar SW, Kaptchuk TJ, et al. 2011. Effects of mindfulness meditation training on anticipatory α modulation in primary somatosensory cortex. *Brain Res Bull* **85:** 96–103.

Kramer MA, Roopun AK, Carrecedo LM, Traub RD, Whittington MA, Kopell NJ. 2008. Rhythm generation through period concatenation in rat somatosensory cortex. *PLoS Comput Biol* **4:** e1000169.

Lopes Da Silva FH, Storm Van Leeuwen W. 1977. The cortical source of the α rhythm. *Neurosci Lett* **6:** 237–241.

Lopes da Silva FH, van Lierop THMT, Schrijer CF, Storm van Leeuwen W. 1973. Organization of thalamic and cortical α rhythms: spectra and coherences. *Electroencephalogr Clin Neurophysiol* **35:** 627–639.

Lopes da Silva FH, Vos JE, Mooibroek J, van Rotterdam A. 1980. Relative contributions of intracortical and thalamo-cortical processes in the generation of α rhythms, revealed by partial coherence analysis. *Electroencephalogr Clin Neurophysiol* **50:** 449–456.

Marescaux C, Vergnes M, Depaulis A. 1992. Genetic absence epilepsy in rats from Strasbourg—a review. *J Neural Transm Suppl* **35:** 37–69.

Nerad L, Bilkey DK. 2005. Ten- to 12-Hz EEG oscillation in the rat hippocampus and rhinal cortex that is modulated by environmental familiarity. *J Neurophysiol* **93:** 1246–1254.

Neunuebel JP, Knierim JJ. 2012. Spatial firing correlates of physiologically distinct cell types of the rat dentate gyrus. *J Neurosci* **32:** 3848–3858.

O'Keefe J. 1976. Place units in the hippocampus of the freely moving rat. *Exp Neurol* **51:** 78–109.

O'Keefe J, Recce ML. 1993. Phase relationship between hippocampal place units and the EEG θ rhythm. *Hippocampus* **3:** 317–330.

Pernía-Andrade AJ, Jonas P. 2014. θ–γ-Modulated synaptic currents in hippocampal granule cells in vivo define a mechanism for network oscillations. *Neuron* **81:** 140–152.

Pfurtscheller G, Aranibar A. 1979. Evaluation of event-related desynchronization (ERD) preceding and following voluntary self-paced movement. *Electroencephalogr Clin Neurophysiol* **46:** 138–146.

Pfurtscheller G, Stancák A Jr, Neuper C. 1996. Event-related synchronization (ERS) in the α band—an electrophysiological correlate of cortical idling: a review. *Int J Psychophysiol* **24:** 39–46.

Rose G, Diamond D, Lynch GS. 1983. Dentate granule cells in the rat hippocampal formation have the behavioral characteristics of θ neurons. *Brain Res* **266:** 29–37.

Roux F, Wibral M, Mohr HM, Singer W, Uhlhaas PJ. 2012. γ-Band activity in human prefrontal cortex codes for the number of relevant items maintained in working memory. *J Neurosci* **32:** 12411–12420.

Skaggs WE, McNaughton BL, Wilson MA, Barnes CA. 1996. θ Phase precession in hippocampal neuronal populations and the compression of temporal sequences. *Hippocampus* **6:** 149–172.

Staley KJ, Otis TS, Mody I. 1992. Membrane properties of dentate gyrus granule cells: comparison of sharp microelectrode and whole-cell recordings. *J Neurophysiol* **67:** 1346–1358.

Steriade M, McCormick DA, Sejnowski TJ. 1993. Thalamocortical oscillations in the sleeping and aroused brain. *Science* **262:** 679–685.

Talley EM, Cribbs LL, Lee JH, Daud A, Perez-Reyes E, Bayliss DA. 1999. Differential distribution of three members of a gene family encoding low voltage-activated (T-type) calcium channels. *J Neurosci* **19:** 1895–1911.

Totah NKB, Kim YB, Homayoun H, Moghaddam B. 2009. Anterior cingulate neurons represent errors and preparatory attention within the same behavioral sequence. *J Neurosci* **29:** 6418–6426.
Totah NKB, Jackson ME, Moghaddam B. 2013. Preparatory attention relies on dynamic interactions between prelimbic cortex and anterior cingulate cortex. *Cereb Cortex* **23:** 729–738.
Varga C, Golshani P, Soltesz I. 2012. Frequency-invariant temporal ordering of interneuronal discharges during hippocampal oscillations in awake mice. *Proc Natl Acad Sci* **109:** E2726–E2734.
Wiest MC, Nicolelis MAL. 2003. Behavioral detection of tactile stimuli during 7–12 Hz cortical oscillations in awake rats. *Nat Neurosci* **6:** 913–914.
Witter MP. 2007. The perforant path: projections from the entorhinal cortex to the dentate gyrus. *Prog Brain Res* **163:** 43–61.
Ylinen A, Soltész I, Bragin A, Penttonen M, Sik A, Buzsáki G. 1995. Intracellular correlates of hippocampal θ rhythm in identified pyramidal cells, granule cells, and basket cells. *Hippocampus* **5:** 78–90.
Youngstrom IA, Strowbridge BW. 2012. Visual landmarks facilitate rodent spatial navigation in virtual reality environments. *Learn Mem* **19:** 84–90.

Received June 25, 2014; accepted in revised form September 10, 2014.